Momentum distributions of electron-positron pairs annihilating at vacancy clusters in Si

M. Hakala,* M. J. Puska,† and R. M. Nieminen‡
Laboratory of Physics, Helsinki University of Technology, FIN-02150 Espoo, Finland
(Received 21 August 1997)

We report calculations of momentum densities of electron-positron pairs annihilating at various vacancy clusters in Si. The densities integrated along one direction, i.e., those corresponding to the spectra measured by the two-dimensional angular correlation of the annihilation radiation method, are shown to be isotropic if the positron is captured by a small vacancy cluster. The densities integrated along two directions correspond to the one-dimensional angular-correlation distribution or the Doppler-broadened annihilation radiation line shape. The characteristic narrowing of these one-dimensional distributions at vacancy clusters is demonstrated. The line-shape parameters S and W describing mainly the annihilations with valence and core electrons, respectively, are calculated and compared quantitatively with experimental data. We find a systematic increase in the S and a decrease in the W parameter as the size of the vacancy increases. [S0163-1829(98)00813-3]

I. INTRODUCTION

Positron annihilation techniques provide several ways to probe atomic-scale defects in materials.[1,2] This is because positrons are trapped by open volume and also by negatively charged defects. The positron lifetime in the material depends on the local electron density at the site of the positron annihilation. At vacancy-type defects, such as small vacancy clusters, the average electron density seen by the positron is reduced, and the positron lifetime is longer than that in the perfect bulk crystal. More information is, however, contained in the momentum density of annihilating electron-positron pairs. It reflects the spatial and momentum (energy) distribution of electrons in the material. For example, in the case of positron trapping the momentum density is strongly sensitive both to the open volume and to the chemical environment of the defect enabling the defect identification.[3] The basic methods to measure momentum densities are the one- and two-dimensional angular correlation of the annihilation radiation (1D-ACAR and 2D-ACAR, respectively) experiments and the detection of the Doppler-broadening of the annihilation rate. Together with the positron lifetime measurement these techniques have been widely used to identify defects in semiconductors.[4–8]

For the elemental and compound semiconductors with diamond or zinc blende lattice structures, the interesting feature in the 2D-ACAR distribution is its anisotropy. The anisotropy is due to the characteristic spatial and momentum distributions of electrons in the perfect bulk or around the defect in question.[9] In the perfect bulk material the 2D-ACAR distributions are rather anisotropic, reflecting the fact that certain valence bands in certain directions in the Brillouin zone do not contribute to the momentum density of annihilating electron-positron pairs. In contrast, for vacancies in semiconductors, the 2D-ACAR distributions are rather isotropic. However, the 2D-ACAR distribution corresponding to aligned divacancies in Si has been shown to have again interesting anisotropies.[10] In Doppler-broadening experiments the characteristic feature is the narrowing of the one-dimensional momentum distribution at vacancy-type defects. Thus, different vacancy agglomerates produce specific momentum distributions and their identification with the 2D-ACAR or the Doppler-broadening method becomes possible.

Recently, Saito and Oshiyama[11] calculated the positron lifetimes for nearest-neighbor vacancy clusters in Si and proposed an assignment to the experimental positron lifetime values. To complement the assignment, we calculate positron annihilation characteristics corresponding to the momentum distributions. First, we show qualitatively the anisotropies of the 2D-ACAR distributions and observe the increasing isotropy as the size of the vacancy cluster increases. We then calculate the momentum distributions corresponding to the Doppler-broadening spectra showing the response to the size of the vacancy cluster. Especially, we determine the line-shape parameters S and W and compare them with existing experimental values. To our knowledge, this is the first time that these parameters are theoretically predicted.

The calculation of the electron-positron momentum distribution requires the determination of the self-consistent electronic structure of the system in question. We obtain the valence electron structure employing the plane-wave pseudopotential method within the density-functional theory. Atomic wave functions are used for the core-electron states. A similar construction of the electron density was recently used by Panda *et al.*[12] when calculating the electron-positron momentum distributions for bulk Si, Ge, and diamond. As systems we consider the perfect bulk lattice and *ideal* vacancy clusters, i.e., the ions surrounding the defect are not allowed to relax from their ideal lattice positions. The omission of the lattice relaxation is justified, because we are mainly interested in the behavior of the positron annihilation characteristics as a function of the open volume of the defect. Moreover, the calculation of the lattice relaxation including the effects of the localized positron is quite sensitive to the theoretical scheme used.[13] The positron states and annihilation characteristics corresponding to these ionic and electronic structures are calculated by taking the electron-positron correlation effects into account. The proper treatment of the correlation effects is important also when calculating the momentum densities of annihilating electron-positron pairs in Si (see, for example, Ref. 12). We use the method by Alatalo *et al.*[6] This method has been previously

used to calculate the core-electron contribution to the momentum distributions[6] and also the valence part in the case of some perfect bulk solids.[14] The present calculation of the line shapes for defects is a new application of the method.

The present paper is organized as follows. The computational methods are explained in Sec. II. In Sec. III the calculated 2D-ACAR distributions for perfect bulk and small vacancy clusters are first discussed. The calculated Doppler spectra and the shape parameters S and W are then presented and compared with experimental data. Section IV concludes the paper.

II. METHOD

The electronic structure for the perfect bulk lattice or for a given defect is calculated within the density-functional theory in the local-density approximation (LDA) (Ref. 15) for the electron exchange and correlation effects. We use norm-conserving nonlocal pseudopotentials[16] with the nonlinear core-valence exchange-correlation scheme[17] and a plane-wave basis to calculate the wave functions for valence electrons. The kinetic-energy cutoff of the plane-wave expansion is 8 Ry, and the supercell size is 64 atom sites. The self-consistent valence-electron densities are obtained by sampling the Brillouin zone with the Monkhorst-Pack[18] $2\times2\times2$ **k**-point mesh (1–4 points depending on the symmetry of the supercell).

The positron wave function is calculated from a one-particle Schrödinger equation for which the potential is constructed using the self-consistent valence electron density and the core electron densities of free atoms.[13] The potential contains the Coulombic and the correlation part. For the positron states localized at defects the so-called conventional scheme is used, in which the finite positron density does not affect the average electron density. The electron density can thus be first determined without the effects of the positron. The correlation potential is calculated using the correlation energy for a delocalized positron in a homogeneous electron gas.[19,20] The conventional scheme is the correct limit of the two-component density-functional theory[20] for a delocalized positron. Due to certain cancellation effects the scheme gives positron densities and annihilation characteristics in good agreement with the appropriate two-component density-functional calculations.[13,21] In practice the positron Schrödinger equation is solved in real space.[22] For a localized positron a Brillouin-zone integration over the lowest lying positron band is used.[21]

We obtain the momentum density $\rho(\mathbf{p})$ of annihilating electron-positron pairs from the electron and positron single-particle wave functions ψ_j and ψ_+, respectively. We use the scheme by Alatalo *et al.*,[6,14] for which

$$\rho(\mathbf{p})=\pi r_e^2 c\sum_j \gamma_j\left|\int d\mathbf{r}\,\exp(-i\mathbf{p}\cdot\mathbf{r})\psi_+(\mathbf{r})\psi_j(\mathbf{r})\right|^2, \quad (1)$$

where $\mathbf{p}$ is the total momentum of the annihilating pair, r_e and c are the classical electron radius and the speed of light, respectively. The enhancement factor γ_j takes into account that the electron density is piled up at the positron due to correlation effects. In the scheme by Alatalo *et al.*[6,14] γ_j depends on the electron state in question,

$$\gamma_j=\lambda_j/\lambda_j^{\mathrm{IPM}}, \quad (2)$$

but not on the momentum proper. Above, the partial annihilation rate λ_j is calculated for each electron state j separately using the LDA (Ref. 23) with the interpolation form by Boroński and Nieminen[19,20] (BN), and the annihilation rate λ_j^{IPM} within the independent particle approximation (IPM). The summation above is over all occupied electron states j. We calculate valence electron states at eight points in the first Brillouin zone of the simple cubic superlattice. The coordinates of the points are given by $(n_1,n_2,n_3)(2\pi/A)$, where $n_1,n_2,n_3 = 0$ or 0.5, and A is the lattice constant of the superlattice. Then we use the fast-Fourier transformation to perform the integration in Eq. (1) (separately) for the eight **k** points. The ensuing momentum density is given in a cubic **p** mesh with a spacing of $1.12\times10^{-3}m_0c$ (m_0 is the electron mass). The core-electron contribution to the momentum density is calculated using free-atom wave functions (for details, see Ref. 6) and added to the valence part.

The 2D-ACAR distribution is obtained by integrating the total momentum density along a given p_z direction:

$$\rho(p_x,p_y)=\int \rho(\mathbf{p})dp_z, \quad (3)$$

and the Doppler spectrum is the one-dimensional momentum distribution

$$\rho(p_z)=\int\int \rho(\mathbf{p})dp_x dp_y, \quad (4)$$

where $p_z=p_L$ is the longitudinal momentum component of the annihilating electron-positron pair. In the following, Eq. (4) is further convoluted with a Gaussian [full width at half maximum (FWHM)$=4.7\times10^{-3}m_0c$] in order to mimic the experimental resolution. The convolution smears the spectrum so that the important information is contained in the relative amounts of annihilations taking place at low- and high-momentum regions ($p_z<10\times10^{-3}m_0c$ and $p_z>10\times10^{-3}m_0c$, respectively). The shape of the Doppler spectrum is monitored by the line-shape parameters S and W.[24] S describes mainly the annihilation with valence electrons whereas W is sensitive to the changes in the core-electron annihilation. In this work we have defined the S parameter as the fraction of annihilations with $p_z\leq2.8\times10^{-3}m_0c$, and the W parameter as the fraction of annihilations within the range of $11\times10^{-3}m_0c\leq p_z\leq20\times10^{-3}m_0c$. These kinds of definitions have also been used in analyzing experimental spectra, for example, in Ref. 25.

Finally, the positron lifetime τ is the inverse of the total annihilation rate λ obtained as

$$\lambda=\int \rho(\mathbf{p})d\mathbf{p}=\pi r_e^2 c\int n_+(\mathbf{r})n_-(\mathbf{r})\gamma(\mathbf{r})d\mathbf{r}, \quad (5)$$

where $n_+(\mathbf{r})$ and $n_-(\mathbf{r})$ are the positron and electron densities, respectively. $\gamma(\mathbf{r})$ is the LDA enhancement factor parametrized by Boroński and Nieminen.[20]

TABLE I. Positron lifetimes (τ) and relative core-electron annihilation rates for the perfect bulk lattice and for the ideal vacancy clusters in Si. λ_c and λ are the core and total annihilation rates, respectively.

System	τ (ps)	λ_c/λ (%)
Bulk	221	2.19
V	254	1.48
V_2	299	0.97
V_3	321	0.79
V_4	330	0.72
V_5	355	0.57

III. RESULTS AND DISCUSSION

A. Positron lifetimes

Our positron lifetime results for the perfect Si and for the ideal vacancy clusters in Si are presented in Table I. We will compare our results with those of the previous study by Saito and Oshiyama[11] and with the experimental data.[25,31,32] The defects have been calculated in the neutral charge state. Actually, the charge state would affect the positron parameters mainly through the ionic relaxation,[26,27] so that in our calculations ignoring the relaxation the charge state is not an important parameter. In the clusters with up to four vacancies the vacancies are adjacent in the same zigzag chain on a [110] plane. The cluster of five vacancies is three dimensional with one central vacancy and its four nearest-neighbor vacancies.

We have used the LDA scheme with the BN enhancement to calculate the annihilation rates. This choice makes the calculations and the interpretation of the results more straightforward than the use of more complicated schemes, such as the generalized gradient approximation (GGA) (Ref. 28) or the correction based on the finite dielectric constant of the semiconductor.[29] The different schemes lead to slightly different absolute positron lifetime values, but the most important features, the differences between the bulk and defect values, are similar in all schemes. The relative magnitude of the core annihilation rate is slightly smaller in the GGA than in the LDA.[6] On the other hand, the pseudopotential construction used in this work for the valence electron density seems to decrease the core rate in comparison with earlier LDA results.[6]

The positron lifetimes for ideal vacancy clusters in Table I are in agreement with those obtained by Saito and Oshiyama,[11] although our calculations are much simpler. We have determined the positron lifetimes for ideal vacancy-type defects using the conventional scheme whereas Saito and Oshiyama performed calculations based on the full two-component density functional theory and thereby obtained self-consistent electron and positron densities. The positron annihilation rates with the core electrons are also given in Table I. For the perfect bulk Si lattice the core contribution is relatively small due to the compact electron core. For the vacancy clusters the positron-core electron overlaps and the ensuing annihilation rates decrease. It should be noted that although we have studied ideal vacancy clusters, our core-electron annihilation rates are remarkably higher than those reported by Saito and Oshiyama for relaxed vacancy clusters. We think that the discrepancy reflects the inadequacy of the two-component scheme by Gilgien *et al.*[30] used by Saito and Oshiyama to describe the electron-positron correlation effects. In the comparison with the conventional scheme the scheme by Gilgien *et al.* has been shown to lead to a much stronger localization for a positron at a defect and therefore to much smaller core annihilation rates.[13] The results of the conventional scheme are in a fair agreement with experiments.[6,13]

Saito and Oshiyama[11] also studied the effects of ionic relaxation by minimizing the total energy. They showed that the ionic relaxation increases the positron lifetime for the small vacancy clusters in comparison with the ideal clusters whereas an opposite effect is found for the larger clusters. However, the influence of the ionic relaxation, perhaps with the exception of the monovacancy, is generally not very large. This is due to a cancellation effect: without the positron the ions surrounding a vacancy defect have a tendency to relax inwards from their ideal lattice positions, but the introduction of the localized positron causes an outward relaxation. This cancellation of the relaxation effects justifies our calculations, which completely ignore the ionic relaxation. On the other hand, it is possible to use the ionic relaxation as a parameter to be determined so that the experimental positron lifetime, or actually the difference between the bulk and defect systems, is reproduced. Then other positron annihilation characteristics could be calculated and compared with experiment.

The positron lifetime of 221 ps calculated for the perfect lattice is longer than $\sim$210–211 ps we obtain by using the same enhancement factor, but employing all-electron methods.[22,26] The agreement is reasonable considering that different computational approximations have been done in the different methods. The lifetime of 221 ps is also in a good agreement with the experimental bulk lifetime of 218 ps.[31] The value of 255 ps for the monovacancy is close to the value of 250 ps obtained for a negatively charged vacancy-phosphorous pair in highly P-doped n-type Si.[32] This defect is isoelectronic with a doubly negative isolated Si vacancy and therefore their ionic relaxations are expected to be similar. For the neutral vacancy-phosphorous pair a longer positron lifetime of 268 ps has been reported.[32] This value is close to the experimental values[31] of about 270 ps for an isolated Si vacancy and somewhat less than the 279 ps calculated for the neutral Si vacancy by Saito *et al.* taking the lattice relaxation into account. One can thus conclude that the ions around the Si vacancy, which is in the neutral charge state with a trapped positron, should relax slightly outwards. The ideal positions of the ions around the Si vacancy, on the other hand, would correspond to a more negative charge state. The positron lifetime given for the ideal divacancy in Table I is slightly shorter than that for a relaxed divacancy calculated by Saito *et al.* The lifetime is also close to the experimental value of 300 ± 5 ps for divacancies.[25]

B. Momentum distributions

Figure 1 shows the calculated 2D-ACAR distributions for the perfect bulk and for the ideal vacancies V_1–V_5 in Si. The integration of the momentum density has been performed with p_z along the [110] direction. The 2D-ACAR distribu-

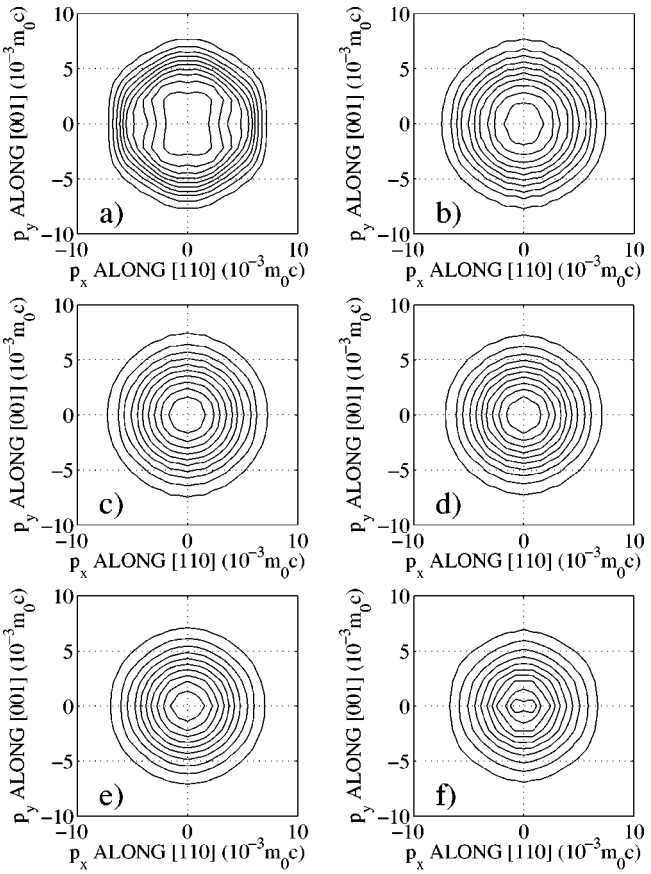

FIG. 1. 2D-ACAR distributions calculated for Si systems and for the [110] plane. (a) Perfect bulk lattice, (b) V_1, (c) V_2, (d) V_3, (e) V_4, and (f) V_5. The contour spacing is one tenth of the maximum value.

tions have been averaged with respect to the different possible orientations of the defect in the crystal. We see that V_1 preserves part of the anisotropy seen in the bulk, but for larger vacancies the distributions become narrower in the [001] direction and very isotropic. The bulklike component in the V_1 map is due to the fact that the positron wave function does not localize totally in the monovacancy but samples also bulklike regions. For the larger vacancy clusters the positron wave function is well localized and isotropic. The isotropy of the V_2 map is in accordance with experimental results.[33] Furthermore, according to the experiments, the various charge states (V_2^0, V_2^{-1}, V_2^{-2}) of the divacancy produce only slightly different 2D-ACAR distributions. The V_3 and V_4 maps are practically isotropic, but in the V_5 map there are more detailed features in the momentum contours. We assume that these features reflect the recovery of the high T_d symmetry of a lattice point.

In the case of the perfect bulk Si [Fig. 1(a)] the valence electron bonding is seen as clear directional anisotropies in the 2D-ACAR momentum distribution. In the Doppler spectra the anisotropies are strongly reduced for the different crystallographic directions. Table II shows the experimental results of Ref. 34 with our calculated ones for the perfect bulk. The calculated values for the monovacancy are also given. For the bulk the present method reproduces the ratios of the S parameters within the experimental error. In contrast, we found a disagreement with experiment by using the

TABLE II. Anisotropy of the characteristic S and W parameters calculated for Si. Experimental values (Ref. 34) are given in square brackets. Before calculating the S and W parameters the theoretical Doppler spectra have been convoluted with a Gaussian with FWHM of $4.7\times10^{-3}m_0c$.

	$S_{hkl}/S_{[100]}$		$W_{hkl}/W_{[100]}$	
hkl	[110]	[111]	[110]	[111]
Bulk	1.008 [1.007(1)]	1.006 [1.005(1)]	1.027	1.054
V_1	1.004	1.003	0.992	1.005

enhancement of Ref. 35 instead of the state-dependent enhancement of Eq. (2): the enhancement of Ref. 35 was found to overestimate the anisotropy considerably. For the monovacancy the characteristic anisotropy diminishes. For V_2 and for the larger vacancy clusters the anisotropy in the S and W parameters vanishes within the calculational accuracy.

The shapes of the Doppler spectra for the perfect bulk lattice and for the ideal vacancies are analyzed in Figs. 2 and 3. Figures 2(a) and 2(b) show the core and valence electron contributions in the Doppler spectrum for the perfect bulk lattice. The calculated Doppler spectra are normalized to unity and given with p_z along the [100], [110], and [111] directions. The anisotropy between the directions is generally rather small, except that there is a bulge at the momentum of about $15\times10^{-3}m_0c$ in the [111] curve, which reflects the symmetry of the perfect Si lattice. The contribution from the annihilations of the positrons with the valence electrons is substantial up to rather high momenta, of $\sim25\times10^{-3}m_0c$.

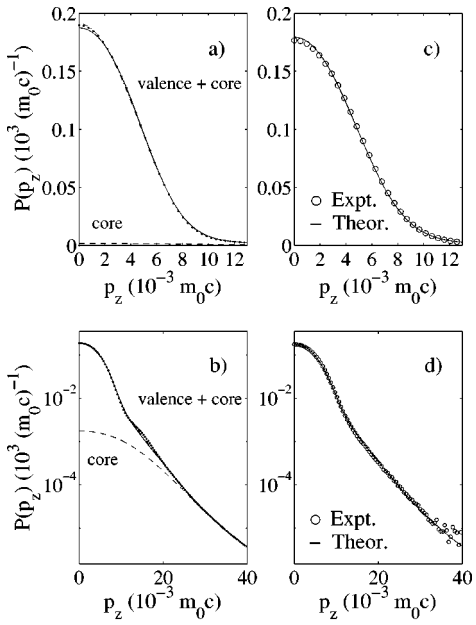

FIG. 2. Positron annihilation probability densities $P(p_z)$ calculated for perfect bulk Si with p_z along the [100], [110], and [111] directions (solid, dash-dotted, and dotted line, respectively): (a) linear, (b) logarithmic scale. Experimental (Ref. 6) (markers) and calculated (lines) positron annihilation probability densities $P(p_z)$ for perfect bulk Si with p_z along the [100] direction: (c) linear, (d) logarithmic scale. The curves have been convoluted with a Gaussian to mimic the experimental resolution.

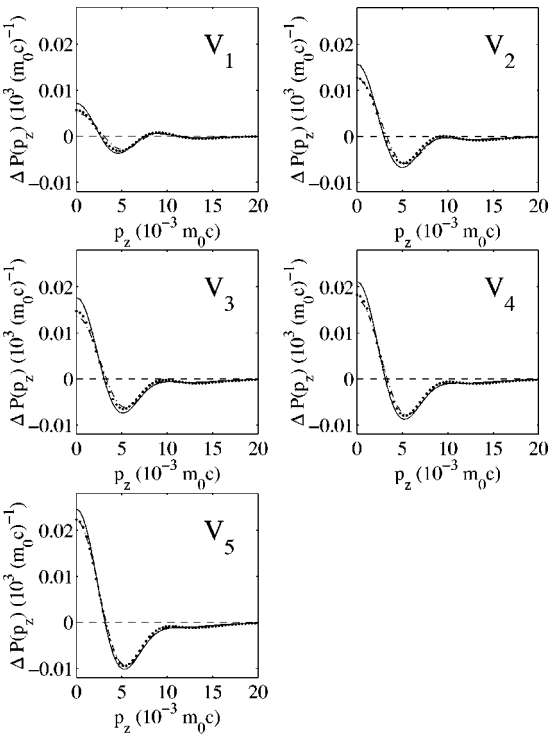

FIG. 3. Differences between positron annihilation probability densities $P(p_z)$ between ideal vacancies V_1–V_5 in Si and perfect bulk Si. Solid, dash-dotted, and dotted lines represent the [100], [110], and [111] directions, respectively. The curves have been convoluted with a Gaussian to mimic the experimental resolution.

This is a result of the small core-electron contribution, which is about 2.2% of the total annihilation rate. The valence electron contribution in the momentum values larger than $10\times10^{-3}m_0c$ explains the directional anisotropy of the W parameter for the perfect bulk and for V_1 in Table II. Figures 2(c) and 2(d) display the comparison between the experimental data of Ref. 6 and the calculated curve with p_z along the [100] direction. The theory reproduces successfully both the high- and the low-momentum parts of the experimental data.

Figure 3 demonstrates the narrowing of the Doppler spectrum as the size of the vacancy cluster increases. We have calculated the Doppler spectra for the different systems and give the differences with respect to the perfect bulk. All difference curves exhibit a similar behavior: the intensity with respect to the bulk is higher below and lower above momenta of about $3\times10^{-3}m_0c$. This kind of narrowing of the spectra reflects the decrease of the average valence electron density (and the effective Fermi momentum) seen by the positron. The small differences between the crystallographic directions are mainly due to the anisotropy in the Doppler spectrum for the perfect bulk. As the size of the vacancy cluster increases, another feature is also evident: the decrease of the intensity at high momenta ($p_z>10\times10^{-3}m_0c$), which is due to the decrease of the relative core annihilation rates (see Table I above).

The narrowing of the Doppler spectrum can be studied quantitatively by the characteristic S and W parameters. In Table III we give the absolute values $S_{\rm bulk}$ and $W_{\rm bulk}$ for the perfect bulk lattice and the relative values $S/S_{\rm bulk}$ and $W/W_{\rm bulk}$ for the defects. The calculated values $S_{\rm bulk}$ and $W_{\rm bulk}$ agree within 6 and 17%, respectively, with the experiments by Kauppinen *et al.*[25] ($S_{\rm bulk}^{\rm exp}=0.5039\pm0.0001$, $W_{\rm bulk}^{\rm exp}=0.02045\pm0.00007$). The results for the ideal vacancy (V) can be compared with those measured for the negatively charged vacancy-phosphorous pair in Si.[36] The comparison is expected to be reasonable because the experimental positron lifetime 250 ps is close to the calculated value of 254 ps. The preliminary experimental results for the $S/S_{\rm bulk}$ and $W/W_{\rm bulk}$ parameters are 1.016 and 0.91, respectively. These are in a fair agreement with the calculated values given in Table III, although one should note that the experimental resolution (FWHM) has been about $6\times10^{-3}m_0c$, i.e., slightly larger than the FWHM of the Gaussian used in the convolution of the theoretical spectrum. In addition, the agreement is good both in shape and magnitude. This means that the substitution of one of the nearest neighbor Si atoms of the vacancy by a P atom should not remarkably influence the momentum distribution around the vacancy. Considering the isolated Si monovacancies, Avalos and Dannefaer[37] have studied electron-irradiated float-zone silicon, and suggest that the $S/S_{\rm bulk}$ value of 1.038 ± 0.003 could be comparable to that for isolated monovacancies. This value is bracketed by our calculation for the ideal monovacancies and divacancies similarly to the corresponding lifetime of 270 ps,[31] which is bracketed by the positron lifetimes for the ideal monovacancy and divacancy.

TABLE III. Characteristic S and W parameters calculated for the perfect bulk lattice and for the ideal vacancy clusters in Si. The momentum component p_z is along the [111] direction. Before calculating the S and W parameters the theoretical Doppler spectra have been convoluted with a Gaussian with FWHM of $4.7\times10^{-3}m_0c$. $S_{\rm val}$ and $S_{B,\rm val}$ have been calculated using the valence electron momentum distributions instead of the total distribution.

System	S/S_B	$S_{\rm val}/S_{B,\rm val}$	W/W_B
Bulk	$S_B=0.5344$	$S_B=0.5410$	$W_B=0.01701$
V	1.018	1.014	0.86
V_2	1.045	1.038	0.72
V_3	1.053	1.045	0.68
V_4	1.067	1.058	0.64
V_5	1.081	1.072	0.59

In the case of divacancy (V_2), two experimental results have been reported. Kauppinen *et al.*[25] give the $S/S_{\rm bulk}$ and $W/W_{\rm bulk}$ values of 1.052 ± 0.003 and 0.78 ± 0.02 for the negative charge state of V_2. The data is measured for proton-implanted low-doped n-type silicon layers. Avalos and Dannefaer,[37] on the other hand, give the $S/S_{\rm bulk}$ value of 1.067 ± 0.002. Our calculation gives the values of 1.045 and 0.72 for the ideal divacancy, in better agreement with the former experimental values. The scatter in the experimental $S/S_{\rm bulk}$ values for the divacancy resembles the scatter in the experimental positron lifetimes for this defect.[25,37] It should be noted that the conventional single-detector spectroscopy was used in Refs. 25 and 37, whereas the coincidence technique[5] was used in Ref. 36.

Figures 4(a)–4(c) summarize the dependence of the lineshape parameters S and W and the positron lifetime on the size of the vacancy cluster. The $S/S_{\rm bulk}$ parameter increases, similarly to the lifetime, as the size of the vacancy cluster

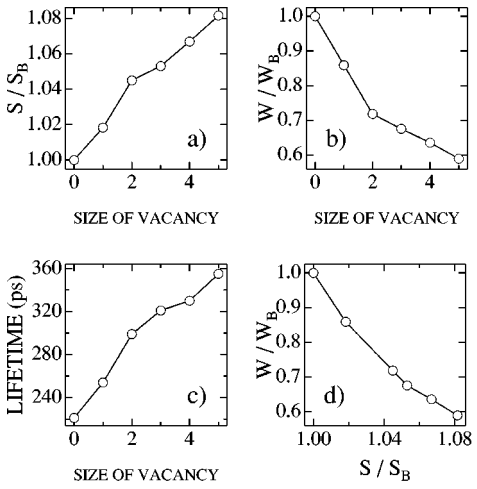

FIG. 4. Positron annihilation characteristics calculated for ideal vacancies in Si as a function of the size of the vacancy cluster: (a) the line-shape parameter S/S_B, (b) the line-shape parameter W/W_B, (c) the positron lifetime τ, (d) W/W_B vs S/S_B. The momentum component p_z is along the [111] direction.

increases, whereas the W/W_{bulk} parameter decreases. In the W/W_{bulk} parameter there is a shift in the rate of decrease as the cluster size becomes larger than that of the divacancy. Due to the anisotropy, another crystal direction than the one used (p_z along [111]) would influence Figs. 4(a) and 4(b) slightly; this effect can be calculated from Table II. If a different window for the W parameter than the interval $(11\text{-}20)\times10^{-3}m_0c$ were used, a different characteristic behavior would be naturally obtained. It is also interesting to see how much the core electron annihilation affects the calculated S parameter values. In Table II we give the parameter S_{val}, which is calculated without the core-electron contribution to the momentum density. This parameter increases less steeply than the one with the core-electron contribution included as the size of the vacancy cluster increases. We conclude that changes in the core-electron annihilation rates when positrons are annihilating at the vacancy clusters in Si do not influence much the shape and magnitude of the Doppler spectrum at low momenta ($p_z<10\times10^{-3}m_0c$). In contrast, Alatalo *et al.*[6] demonstrated that the high-momentum region ($p_z>10\times10^{-3}m_0c$) is strongly dependent on the magnitude of the core annihilation. Finally, Fig. 4(d) shows the almost linear relation between the S/S_{bulk} and W/W_{bulk} parameters for the different vacancy clusters. Vacancies and vacancy clusters decorated with impurities in the material can produce significantly different S/S_{bulk} and W/W_{bulk} parameters compared to this linear relation. Therefore, the present results may be useful in guiding the experimental identification between the clean vacancy clusters and the vacancy clusters decorated with impurities.

IV. CONCLUSIONS

We have calculated electron-positron momentum distributions for ideal vacancy clusters in Si. For unoriented vacancy clusters consisting of 2–5 vacancies the 2D-ACAR distributions are very isotropic along different crystallographic directions. We have calculated the characteristic valence (S) and core (W) annihilation parameters for the ideal systems. The results for the monovacancy and divacancy agree well with the experimental data. The S and W parameters are strongly sensitive to the size of the vacancy cluster, which confirms that the Doppler-broadening spectroscopy is effective in defect studies. However, one should emphasize that the comparisons of the whole momentum distributions give more information than the comparisons of the integrated S and W parameters.

ACKNOWLEDGMENTS

We thank P. Hautojärvi and K. Saarinen for discussions and H. Kauppinen for providing experimental Doppler-broadening data for Si. We would also like to thank S. Pöykkö for assistance in the plane-wave pseudopotential calculations.

*Electronic address: Mikko.Hakala@hut.fi
†Electronic address: Martti.Puska@hut.fi
‡Electronic address: Risto.Nieminen@hut.fi

[1] *Positron Spectroscopy of Solids*, edited by A. Dupasquier and A. P. Mills, Jr. (IOS, Amsterdam, 1995).
[2] M. J. Puska and R. M. Nieminen, Rev. Mod. Phys. **66**, 841 (1994).
[3] S. Berko in *Momentum Distributions*, edited by R. N. Silver and P. E. School (Plenum, New York, 1989), p. 273.
[4] R. Ambigapathy, A. A. Manuel, P. Hautojärvi, K. Saarinen, and C. Corbet, Phys. Rev. B **50**, 2188 (1994).
[5] M. Alatalo, H. Kauppinen, K. Saarinen, M. J. Puska, J. Mäkinen, P. Hautojärvi, and R. M. Nieminen, Phys. Rev. B **51**, 4176 (1995).
[6] M. Alatalo, B. Barbiellini, M. Hakala, H. Kauppinen, T. Korhonen, M. J. Puska, K. Saarinen, P. Hautojärvi, and R. M. Nieminen, Phys. Rev. B **54**, 2397 (1996).
[7] K. Saarinen, T. Laine, K. Skog, J. Mäkinen, P. Hautojärvi, K. Rakennus, P. Uusimaa, A. Salokatve, and M. Pessa, Phys. Rev. Lett. **77**, 3407 (1996).
[8] K. Saarinen, P. Hautojärvi, and C. Corbel, in *Identification of Defects in Semiconductors*, edited by M. Stavola (Academic, New York, in press).
[9] M. Saito, A. Oshiyama, and S. Tanigawa, Phys. Rev. B **44**, 10 601 (1991).
[10] Z. Tang, M. Hasegawa, T. Chiba, M. Saito, A. Kawasuso, Z. Q. Li, R. T. Fu, T. Akahane, Y. Kawazoe, and S. Yamaguchi, Phys. Rev. Lett. **78**, 2236 (1997).
[11] M. Saito and A. Oshiyama, Phys. Rev. B **53**, 7810 (1996).
[12] B. K. Panda, S. Fung, and C. D. Beling, Phys. Rev. B **53**, 1251 (1996).
[13] M. J. Puska, A. P. Seitsonen, and R. M. Nieminen, Phys. Rev. B **52**, 10 947 (1995).
[14] B. Barbiellini, M. Hakala, M. J. Puska, and R. M. Nieminen, Phys. Rev. B **56**, 7136 (1997).
[15] D. M. Ceperley and B. J. Alder, Phys. Rev. Lett. **45**, 566 (1980); J. Perdew and A. Zunger, Phys. Rev. B **23**, 5048 (1981).
[16] G. B. Bachelet, D. R. Hamann, and M. Schlüter, Phys. Rev. B **26**, 4199 (1982); D. R. Hamann, Bull. Am. Phys. Soc. **33**, 803 (1988).

[17] S. G. Louie, S. Froyen, and M. L. Cohen, Phys. Rev. B **26**, 1738 (1982).
[18] H. J. Monkhorst and J. D. Pack, Phys. Rev. B **13**, 5188 (1976).
[19] J. Arponen and E. Pajanne, Ann. Phys. (N.Y.) **121**, 343 (1979); J. Phys. F **9**, 2359 (1979).
[20] E. Boroński and R. M. Nieminen, Phys. Rev. B **34**, 3820 (1986).
[21] T. Korhonen, M. J. Puska, and R. M. Nieminen, Phys. Rev. B **54**, 15 016 (1996).
[22] A. P. Seitsonen, M. J. Puska, and R. M. Nieminen, Phys. Rev. B **51**, 14 057 (1995).
[23] K. O. Jensen, J. Phys.: Condens. Matter **1**, 10 595 (1989).
[24] P. Hautojärvi and C. Corbel, in *Positron Spectroscopy of Solids* (Ref. 1).
[25] H. Kauppinen, C. Corbel, K. Skog, K. Saarinen, T. Laine, P. Hautojärvi, P. Desgarding, and E. Ntsoenzok, Phys. Rev. B **55**, 9598 (1997).
[26] M. J. Puska, O. Jepsen, O. Gunnarsson, and R. M. Nieminen, Phys. Rev. B **34**, 2695 (1986).
[27] M. Alatalo, M. J. Puska, and R. M. Nieminen, J. Phys.: Condens. Matter **5**, L307 (1993).
[28] B. Barbiellini, M. J. Puska, T. Torsti, and R. M. Nieminen, Phys. Rev. B **51**, 7341 (1995); B. Barbiellini, M. J. Puska, T. Korhonen, A. Harju, T. Torsti, and R. M. Nieminen, *ibid.* **53**, 16 201 (1996).
[29] M. Puska, S. Mäkinen, M. Manninen, and R. M. Nieminen, Phys. Rev. B **39**, 7666 (1989).
[30] L. Gilgien, G. Galli, G. Gygi, and R. Car, Phys. Rev. Lett. **72**, 3214 (1994).
[31] S. Dannefaer, in *Proceedings of Defect Control in Semiconductors*, edited by K. Sumino (North-Holland, Amsterdam, 1989), p. 1561.
[32] J. Mäkinen, P. Hautojärvi, and C. Corbel, J. Phys.: Condens. Matter **4**, 5137 (1992).
[33] M. Hasegawa, A. Kawasuso, T. Chiba, T. Akahane, M. Suezawa, S. Yamaguchi, and K. Sumino, Appl. Phys. A: Solids Surf. **61**, 65 (1995).
[34] S. Dannefaer, W. Puff, and D. Kerr, Phys. Rev. B **55**, 2182 (1997).
[35] S. Daniuk, G. Kontrym-Sznajd, J. Mayers, A. Rubaszek, H. Stachowiak, P.A. Walters, and R. N. West, in *Positron Annihilation*, Proceedings ICPA7, edited by P. C. Jain, R. M. Singru, and K. P. Gopinathan (World Scientific, Singapore, 1985) p. 43; S. Daniuk, G. Kontrym-Sznajd, A. Rubaszek, H. Stachowiak, P. A. Walters, and R. N. West, J. Phys. F **17**, 1365 (1987).
[36] H. Kauppinen and K. Saarinen (private communication).
[37] V. Avalos and S. Dannefaer, Phys. Rev. B **54**, 1724 (1996).